Journal of Medicinal Chemistry

Article

Comparative Epitope Mapping with Saturation Transfer Difference NMR of Sialyl Lewis Compounds and Derivatives Bound to a Monoclonal Antibody

Lars Herfurth, Beat Ernst, Beatrice Wagner, Daniel Ricklin, Daniel S. Strasser, John L. Magnani, Andrew J. Benie, and Thomas Peters

J. Med. Chem., **2005**, 48 (22), 6879-6886• DOI: 10.1021/jm0502687 • Publication Date (Web): 30 September 2005

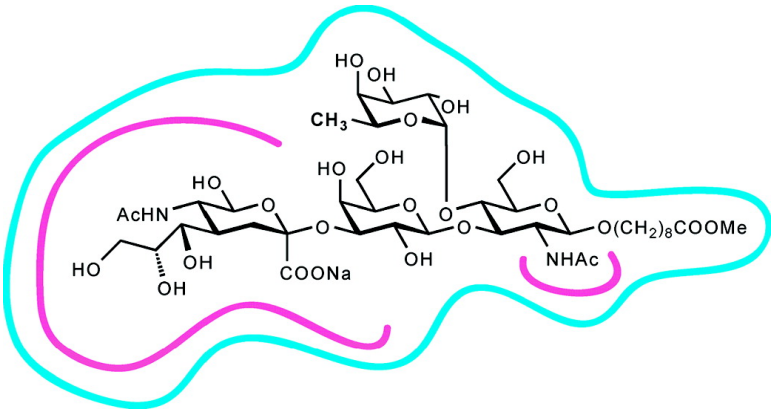

More About This Article

Additional resources and features associated with this article are available within the HTML version:

- Supporting Information
- Links to the 2 articles that cite this article, as of the time of this article download
- Access to high resolution figures
- Links to articles and content related to this article
- Copyright permission to reproduce figures and/or text from this article

View the Full Text HTML

Journal of Medicinal Chemistry is published by the American Chemical Society. 1155 Sixteenth Street N.W., Washington, DC 20036

Comparative Epitope Mapping with Saturation Transfer Difference NMR of Sialyl Lewis^a Compounds and Derivatives Bound to a Monoclonal Antibody

Lars Herfurth,[†] Beat Ernst,*[,‡] Beatrice Wagner,[‡] Daniel Ricklin,[‡] Daniel S. Strasser,[‡] John L. Magnani,[§] Andrew J. Benie,[†] and Thomas Peters*[,†]

Institute of Chemistry, University of Lübeck, Ratzeburger Allee 160, 23538 Lübeck, Germany, Institute of Molecular Pharmacy, University of Basel, Klingelbergstasse 50, CH-4046 Basel, Switzerland, and GlycoTech Corporation, 7860 Beechcraft Avenue, Gaithersburg, Maryland 20879

Received March 23, 2005

The monoclonal antibody GSLA-2 recognizes the sialyl Lewis^a (sLe^a) epitope, which has an increased occurrence on mucin type glycoproteins of patients with colorectal carcinoma. GSLA-2 is therefore used in tumor diagnosis. To advance the understanding of this highly specific molecular recognition reaction, we have analyzed the binding epitope of sLe^a at atomic resolution using saturation transfer difference NMR. To compare, the binding epitopes of sialyl Lewis^x (sLe^x) and of four synthetic derivatives of sLe^a were explored. Surface plasmon resonance experiments furnished thermodynamic and kinetic data. It is observed that all pyranose rings of sLe^a are in contact with the protein surface, with the neuramic acid residue receiving the largest fraction of saturation transfer. In contrast, sLe^x binds very weakly, though specifically to GSLA-2, with a different binding epitope. This study provides a comprehensive picture of the recognition sLe^a and explains the exquisite specificity of the antibody.

Introduction

Tumor growth normally is associated with the presence of tumor-associated antigens that may serve as targets for therapy or diagnosis. Today, the use of monoclonal antibodies for diagnostic purposes is well established, and therapeutic applications are on the rise.[1] A better understanding of antibody−antigen recognition will certainly support these applications. From X-ray diffraction studies, the structures of many antibody−antigen complexes have become available. Among these, antibodies recognizing carbohydrate epitopes have turned out to be challenging targets for crystallization.[2] In solution, the analysis of transfer NOEs has furnished bioactive conformations of carbohydrate antigens bound to monoclonal antibodies,[3−5] and more recently, STD NMR experiments[6−9] have been used to map the binding epitopes of carbohydrate antigens at atomic resolution.[5,10,11] The monoclonal antibody GSLA-2 detects the tumor-associated antigen CA19-9,[12−15] which comprises the sLe^a epitope in sera from patients with pancreatic and gastrointestinal cancer.[16,17] An automated cancer diagnostic assay based on GSLA-2 has a proven clinical performance and demonstrates good correlation with the approved CA19-9 assay.[18]

The sLe^a epitope is characterized by a fucose and a sialic acid residue attached to the type 2 Lac*N*Ac core, whereas the sLe^x epitope contains the type 1 core structure. This causes a structural similarity of the two epitopes that was first discussed by Lemieux and coworkers[19] and is illustrated in Figure 1. The spatial positioning of sialic acid, fucose, and galactose creates a common three-dimensional motif that is shared by both sLe^a and sLe^x.[20] Most monoclonal antibodies can distinguish between sLe^a and sLe^x. A rare exception is the antibody HECA 452, which along with E-selectin binds with significant affinity to both structures.

The monoclonal antibody GSLA-2 readily discriminates between sLe^a and sLe^x. sLe^x is said not to be recognized by GSLA-2. To understand the basis for this discrimination, the binding epitopes of GSLA-2 ligands need to be analyzed at an atomic resolution. We have employed a combination of STD NMR experiments and surface plasmon resonance experiments (Biacore)[21−23] in order to study this problem.

STD NMR experiments have been introduced[6] to detect and characterize the binding of ligands to receptor proteins.[9] Saturation transfer has initially been used to characterize binding in tightly bound complexes and to follow the kinetics of exchange processes.[24,25] Saturation transfer has also been applied in the analysis of the binding of carbohydrate ligands to proteins.[26,27] However, the enormous potential of saturation transfer NMR experiments to screen compound mixtures for binding activity was not realized until recently.[6] The experimental protocol is based on the transfer of saturation from the protein to bound ligands that then exchange into solution to utilize the free ligand signals for detection. Subtracting a spectrum of the saturated protein from that obtained in the absence of protein saturation produces a difference spectrum where only the signals of the ligand(s) remain. The irradiation frequency for protein saturation is set to a value where only protein resonances and no ligand resonances occur. Therefore, in the on-resonance experiment a selective saturation of the protein is achieved. To achieve the desired selectivity and to avoid sideband irradiation,

* To whom correspondence should be addressed. For B.E.: phone, +41-61-267-1551; fax, +41-61-267-1552; e-mail, beat.ernst@unibas.ch. For T.P.: phone, +49-451-500-4230; fax, +49-451-500-4241; e-mail, thomas.peters@chemie.uni-luebeck.de.
[†] University of Lübeck.
[‡] University of Basel.
[§] GlycoTech Corporation.

10.1021/jm0502687 CCC: $30.25
Published on Web 09/30/2005

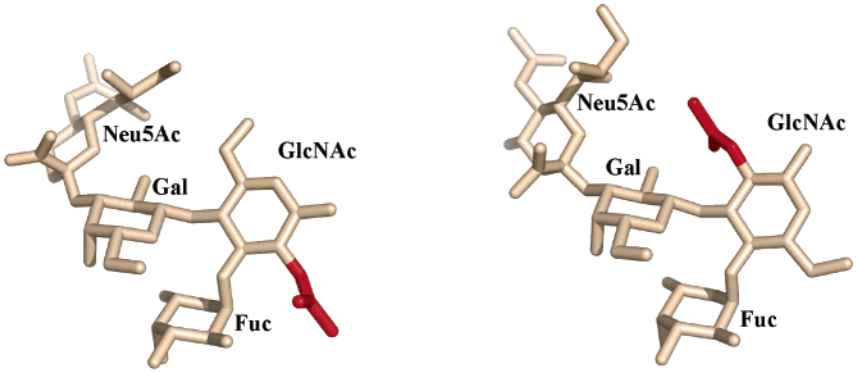

sLe^x **sLe^a**

Figure 1. Structural similarity of sLe^a (right) and sLe^x (left). The *N*Ac (red) and the CH_2OH groups (opposite the *N*Ac group) of the GlcNAc moiety "change places". The models were generated with the program SYBYL (Tripos Inc.) using coordinates of published conformational analyses.[31,34,35] The images were produced with the program PyMOL (http://www.delanoscientific.com/). It is well established that the Le^a and Le^x trisaccharide core structures are rather rigid[36,37] and thus not altered by the attachment of a sialic acid residue in the 3-position of galactose.[34,36−40] The sLe^x tetrasaccharide is shown in its bioactive conformation when bound to E-selectin.[31] The sLe^a tetrasaccharide is shown in a similar conformation (structure **2** of SLNFPII in Table 3 of ref 34) that has been described to be one of the major conformations in solution.[34,35] For clarity, neither the spacer nor the hydrogen atoms are shown. Also, heavy atoms are not discriminated by color.

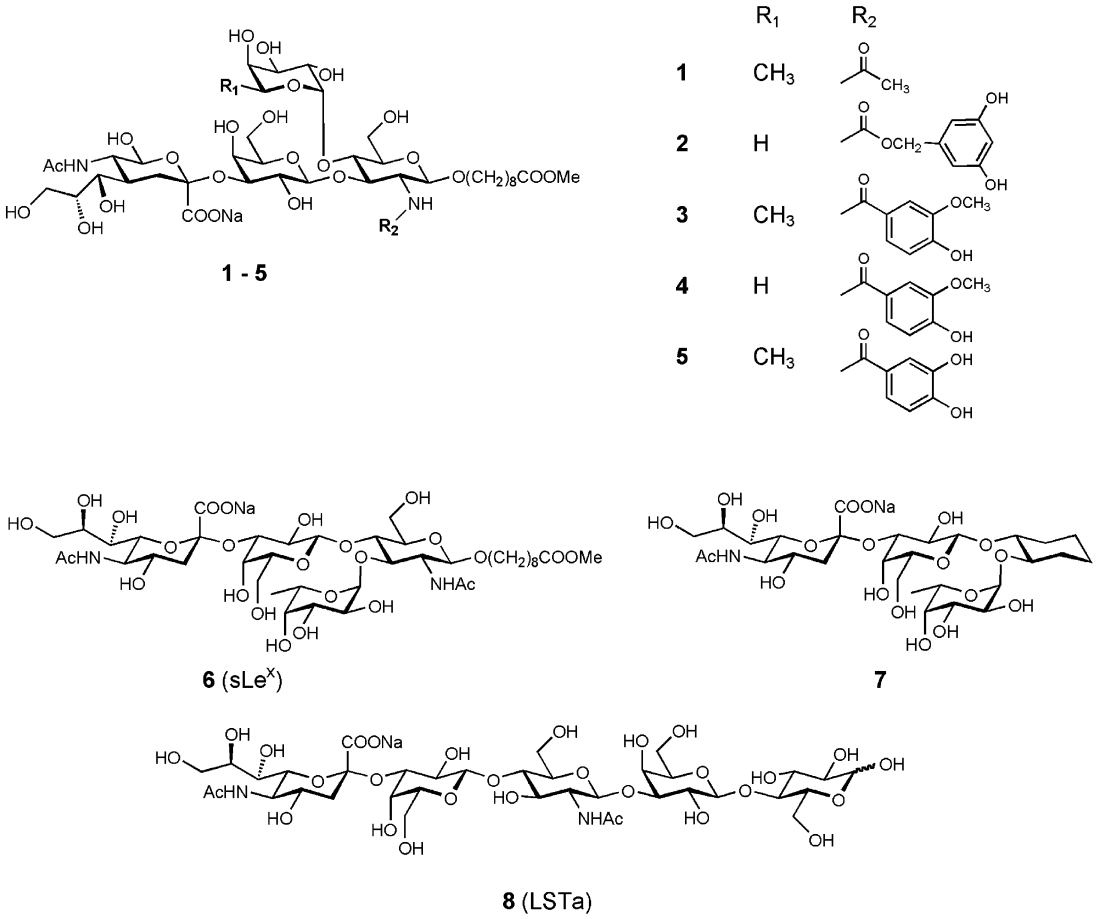

Figure 2. Formulas of the compounds investigated. The chemoenzymatic syntheses of the oligosaccharides were performed according to the following superscripted references: sLe^a (**1**),[41] **2**,[42] **3** and **4**,[43] **5**,[42] and sLe^x (**6**) and **7**.[44] LSTa (**8**) was obtained commercially.

shaped pulses are employed for the saturation of the protein signals. The method not only discriminates binding from nonbinding molecules but more importantly allows the determination of binding epitopes at atomic resolution.[8] Recently, it has been reported that on the basis of structural data, e.g., from X-ray analysis or modeling, experimental STD NMR data can be subjected to a full relaxation matrix analysis that also includes the exchange kinetics of the binding reaction.[28] Such a treatment allows the prediction and optimization of the conformation and orientation of the ligand in the binding pocket of the receptor protein.[29,30]

Here, we have studied a set of compounds that are related to sLe^a to inspect the requirements for binding

Table 1. Dissociation Constants K_D from Surface Plasmon Resonance Experiments (Equilibrium Analysis) Performed at 298 K with mAb GSLA-2 Immobilized on a CM5 Chip[a]

	ligand						
	sLe^a	sLe^x	LSTa	**2**	**3**	**4**	**5**
K_D (μM)	4 ± 2	nd[b]	73 ± 5	211 ± 11	114 ± 11	606 ± 266[c]	46 ± 2

[a] The data for sLe^a were averaged from five independent experiments. For LSTa and compounds **2**−**5** four independent experiments were performed. From the molecular weight of sLe^a (MW = 1012.99 g mol^{-1}) a maximum RU value of 243 is calculated compared to a maximum value of 124 from the experimental data, substantiating the assumption of a simple 1:1 binding model. [b] For sLe^x and compound **7** (not shown in this table), no binding affinity was detected. [c] For compound **4** the significant error is due to the large K_D value. At this affinity, the titration would have to be performed up to about 6 mM in order to obtain saturation. The highest concentration used in the titration of **4** was 800 μM.

to GSLA-2. The set of compounds employed in this study is shown in Figure 2. This analysis aims to establish a structure−binding relationship without any prior knowledge of the three-dimensional structure of the antibody.

Results

The binding of sLe^a and derivatives (Figure 2) to GSLA-2 was studied using STD NMR experiments and surface plasmon resonance (Biacore). The Biacore analysis yielded thermodynamic and kinetic data, whereas the STD NMR study revealed the binding epitopes of the ligands at atomic resolution.

Biacore Experiments. The dissociation constants K_D for sLe^a and its derivatives are summarized in Table 1 showing that sLe^a has the highest affinity for GSLA-2. Any structural changes to the molecule lead to a decreased binding affinity. For sLe^x and for compound **7**, where the Glc*N*Ac residue had been substituted with a cyclohexanediol ring, no binding activity was observed.

The dissociation constants of all ligands except for sLe^a were in the high micromolar range with off-rate constants k_{off} that were beyond the kinetics resolution of the Biacore instrument. Only for sLe^a was a kinetics analysis possible, although at the kinetics resolution limit of the instrument. Figure 3 shows those sensorgrams that were used for the kinetics analysis. The curves were globally fitted to a Langmuir 1:1 binding model employing standard Biacore software. The sensorgrams in Figure 3B were obtained at 0.2, 0.5, 1.0, 2.0, and 5.0 μM ligand concentrations. The sensorgrams in Figure 3A lack the sensorgram at 2.0 μM ligand concentration, which does not return to the baseline. It is found that the binding of sLe^a is characterized by a k_{off} value of about 0.5 s^{-1} and a k_{on} value of about 10^5 M^{-1} s^{-1}. From the k_{off} value a half-life of the bound state of 1.4 s was calculated.

STD NMR Experiments with sLe^a and GSLA-2. For the STD NMR experiments a solution containing a 20-fold molar excess of sLe^a over GSLA-2 was used. The concentration of binding sites was 6.4 μM, and the experiments were performed at 290 and 310 K. At 310 K the signals for the two *N*-acetyl methyl groups of the Glc*N*Ac and the Neu5Ac moieties were not resolved as individual signals. On the other hand, the anomeric proton and H5 of the fucose residue were not obscured by the residual HDO signal at this temperature. At 290 K the *N*-acetyl methyl groups were well separated but H1 and H5 of the fucose residue were buried underneath the HDO signal. For the on-resonance spectra, irradiation frequencies of either 0.4 or 6.7 ppm were used. It is observed that all pyranose rings of sLe^a receive significant saturation transfer. In contrast, the O(CH$_2$)$_8$-COOMe reducing end substituent only receives little saturation. The relative STD intensities of protons of the pyranose rings are summarized in Table 2. It is obvious that the STD effects obtained from saturating the aromatic amino acid residues at 6.7 ppm are different from those resulting from saturation of aliphatic side chain protons at 0.4 ppm. H1 of Gal and H1 of Glc*N*Ac as well as H3 of Gal and H3 of Glc*N*Ac have almost identical chemical shifts, and therefore, a separate analysis of the corresponding STD effects is impossible. Comparison of the relative STD intensities obtained at 290 and 310 K reveals a temperature dependence of the data. At both temperatures, the *N*-acetyl groups of the Neu5Ac residues receive the largest relative amount of saturation transfer.

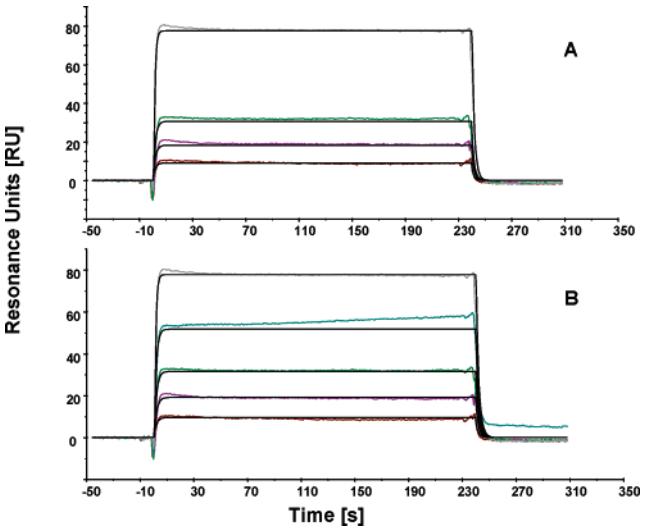

Figure 3. Biacore sensorgrams of sLe^a binding to GSLA-2 (immobilized; see Experimental Section for details) for which a kinetics analysis was performed. Sensorgrams were fitted to a Langmuir 1:1 binding model utilizing standard Biacore software in the global fitting mode. (A) The concentrations of sLe^a were (from bottom to top) 0.2, 0.5, 1.0, 2.0, and 5.0 μM. The global fit yielded the following parameters: $K_A = 1.7 \times 10^5$ M^{-1}, $K_D = 5.9 \times 10^{-6}$ M, RU$_{max}$ = 173, $k_{off} = 0.54$ s^{-1}, $k_{on} = 9.2 \times 10^4$ M^{-1} s^{-1}, $\chi^2 = 9$. (B) The ligand concentrations were (from bottom to top) 0.2, 0.5, 1.0, and 5.0 μM. The global fit yielded the following parameters: $K_A = 2.3 \times 10^5$ M^{-1}, $K_D = 4.3 \times 10^{-6}$ M, RU$_{max}$ = 149, $k_{off} = 0.48$ s^{-1}, $k_{on} = 1.1 \times 10^5$ M^{-1} s^{-1}, $\chi^2 = 11$. The data show that the association process of sLe^a and GSLA-2 is slower than expected for a diffusion-controlled process. From k_{off} a half-life of 1.4 s is calculated. The K_D values derived from this kinetics analysis compare well with the data in Table 1.

STD NMR Experiments and Transferred NOE Analyses with sLe^x and GSLA-2. For the STD NMR experiments samples with different ratios of sLe^x to GSLA-2 were prepared. At low ratios, i.e., 12:1 and 25:1, only one signal is observed at 310 K for the two *N*-acetyl groups. At higher ratios of 100:1 and for free sLe^x, two signals are observed that are separated by about 0.1−0.2 ppm. This effect is due to chemical exchange. STD spectra were obtained at a ratio of 100:1 of sLe^x to GSLA-2. Weak STD effects are observed for each pyranose unit of sLe^x (Table 2). From Table 2 it is obvious that the neuramic acid residue of sLe^x is most

Table 2. Relative STD Intensities for sLe^a and sLe^x Bound to GSLA-2 at 500 MHz[a]

T (K), *F* (ppm)	H1 (Fuc)	H5 (Fuc)	H1 (Gal, GlcNAc)	H3 (Gal, GlcNAc)	H6proS (GlcNAc)	H4 (Gal)	H4 (Fuc)	H5 (GlcNAc), H7 (Neu5Ac)	H2 (Gal)	H3eq (Neu5Ac)	NAc (GlcNAc)	NAc (Neu5Ac)	H3ax (Neu5Ac)	H6 (Fuc)
							sLe^a							
310, 0.4	43	49	45	49	38	43	48	43	56	47	100*	100*	38	62
310, 6.7	73	73	68	69	53	59	62	53	73	44	100*	100*	53	43
290, 0.4	nd	nd	27	27	22	19	29	27	22	31	41	59	40	58
290, 6.7	nd	nd	65	61	45	38	49	43	37	nd	40	60	nd	16
							sLex							
310, 7.2	16	21	0	23	24	18	10	33	47	26	0	100	56	25

[a] sLe^a: The STD NMR values are normalized using *N*-acetyl groups as a reference. At 310 K, the signals for the *N*-acetyl groups are not separated. The values given are the sum of the two signals. Therefore, at 290 K the STD NMR signals are also normalized using the sum of the STD NMR factors of the two *N*-acetyl groups as a reference (signals marked with an asterisk). The saturation frequency *F* for the on-resonance spectrum was 0.4 or 6.7 ppm, and for the off-resonance spectrum it was 40 ppm. The saturation time was 3 s, and 1K scans were obtained. The data suggest that the binding mode may slightly alter with the temperature. sLe^x: The STD values are normalized using the *N*-acetyl group of Neu5Ac as a reference. The saturation frequency for the on-resonance spectrum was 7.2 ppm, and for the off-resonance spectrum it was 40 ppm. The saturation time was 1.6 s, and 1280 scans were collected. In contrast to sLe^a, no saturation transfer is observed for the *N*-acetyl group of the Glc*N*Ac unit.

important for binding. Because the binding affinity of sLe^x was too low to be observed in the Biacore experiment, we analyzed NOESY experiments for the transferred nuclear Overhauser effect of sLe^x in the presence of GSLA-2 to substantiate its low binding affinity. At 500 MHz NOEs for free sLe^x were negative, as has been previously described.[31] Therefore, at this field strength binding cannot be detected on the basis of a change of the sign of the NOEs, and the acquisition of NOE buildup curves and their analysis for a transferred NOE component were necessary. The buildup curves show that the maximum NOE is at mixing times between 600 and 800 ms for sLe^x in the presence of GSLA-2, compared to a maximum NOE at mixing times between 800 and 1000 ms for free sLe^x. This change indicates the presence of a transferred NOE component to the NOE in the presence of antibody and is thus a clear sign of (weak) binding of sLe^x to GSLA-2. A detailed analysis of the bound conformation of sLe^x was not attempted because of the small differences between the NOE buildup curves.

Competitive STD NMR and NOE Experiments with sLe^x and sLe^a in the Presence of GSLA-2. The mode of binding of sLe^a and sLe^x was further investigated by competitive STD NMR and NOE experiments. For the NOE experiments, a field strength of 360 MHz was chosen in order to observe positive NOEs for free sLe^a and sLe^x. At this field strength, for both tetrasaccharides the presence of the transferred NOE contribution to the NOE results in the observation of a negative NOE, which unambiguously indicates binding of the saccharides to the antibody. A titration of a sample of sLe^x and GSLA-2 with sLe^a gives a series of NOE spectra where the sign of the cross-peaks of sLe^a gradually changes from positive to negative (Figure 4). At each titration point, STD spectra were also obtained. The STD spectrum (Figure 5B) and a reference spectrum (Figure 5A) at a ratio of sLe^a/sLe^x/GSLA-2 of 73:100:1 indicate that at this point only signals from sLe^a are observed because sLe^x has been completely displaced from the binding pocket of GSLA-2. The enlarged regions in Figure 5 show two signals, H1 of fucose and H3ax of Neu5Ac, that allow an easy distinction between sLe^a and sLe^x.

STD NMR Experiments with Tetrasaccharides 2−4 and GSLA-2. For the sLe^a derivatives **2**−**4** STD

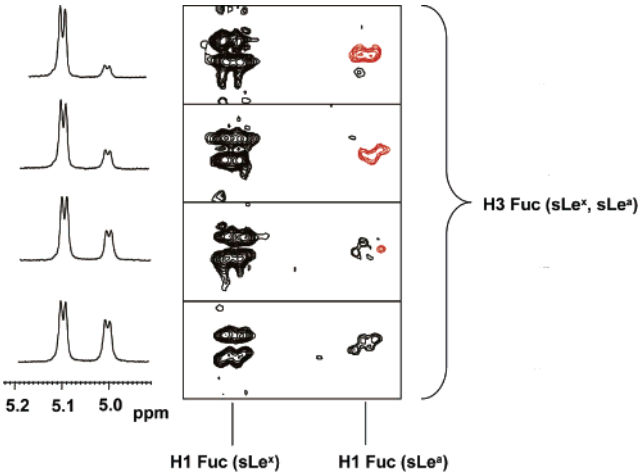

Figure 4. Portions of the NOE spectra obtained at 360 MHz and 300 K for a mixture of sLe^a, sLe^x, and GSLA-2. For each spectrum a mixing time of 400 ms was used. The ratio of sLe^a/sLe^x/GSLA-2 was (top) 16:100:1, (second from top) 26:100:1, (third from top) 53:100:1, and (bottom) 73:100:1. The cross-peak shown is the one between H1 and H3 of fucose. sLe^x gives negative cross-peaks (black) at 360 MHz in the presence of GSLA-2 due to transferred NOEs. The sign of the cross-peaks for sLe^a change from positive (red) to negative at ratios above approximately 50:100:1, indicating competition with sLe^x for the same binding site of the antibody. For reference, on the left the anomeric protons H1 of fucose are shown during the titration.

NMR experiments were performed for a 20- to 200-fold molar excess of ligand over GSLA-2. For these compounds only the STD effects of the protons of the aromatic substituents at the 2-position of the Glc*N*Ac ring, of H1 and H6 of fucose, and of H3eq, H3ax and the *N*-acetyl group of Neu5Ac were analyzed because of severe signal overlap in the spectral region between 3.3 and 4.1 ppm. For comparison, the STD effects were normalized using the signal of the methyl group of the *N*-acetyl side chain of the Neu5Ac unit as a reference. A comparison of the STD data shows that the pattern of saturation transfer is very similar for tetrasaccharides **3**−**5**. An inspection of the region between 3.3 and 4.1 ppm reveals no significant differences between the compounds investigated. Qualitatively, it is observed that the relative extent of saturation transfer to protons of the Gal and the modified Glc*N*Ac unit is less efficient than for the Neu5Ac and Fuc units, as has been

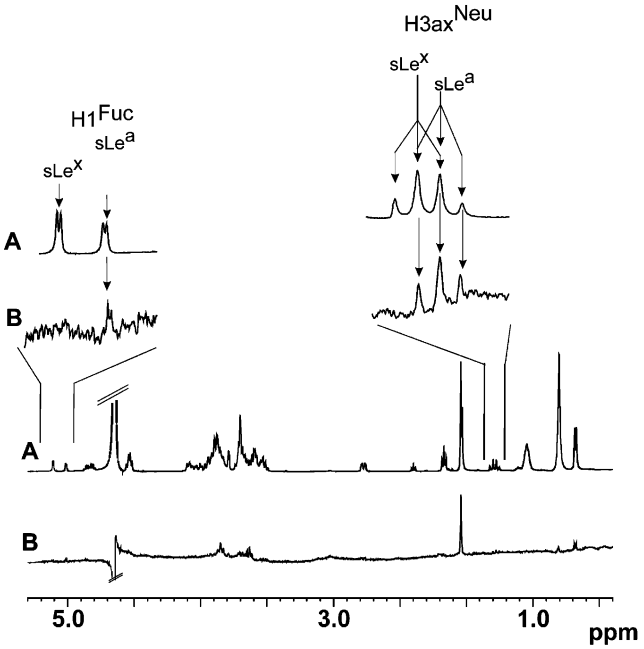

Figure 5. STD spectra of a mixture of sLe^x and sLe^a in the presence of GSLA-2 at a ratio of 100:73:1 sLe^x/sLe^a/GSLA-2 at 500 MHz in D_2O. The on-resonance frequency was 7.2 ppm, and the off-resonance frequency was 40 ppm. The saturation pulse was 1 s in duration. Spectrum A shows the ^{1}H NMR for the reference, and spectrum B is the STD spectrum. The insets show the protons H1 of fucose and H3ax of Neu5Ac. These protons have different chemical shifts in sLe^a and sLe^x and were used to detect differential binding of the two tetrasaccharides.

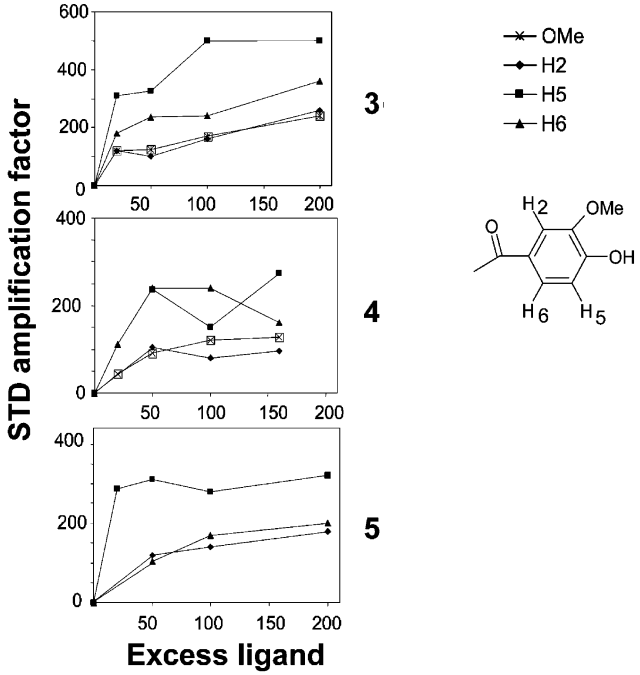

Figure 6. STD amplification factors (see Experimental Section) of compounds **3**−**5** as a function of excess ligand. It is seen that the saturation transfer to H5 in the *N*-acyl side chain is most pronounced in each of the three tetrasaccharides. For compound **5**, only three curves are shown because it contains two free OH groups instead of the OH and OMe groups in compounds **3** and **4**.

described above for sLe^x (Table 2). The *N*-acetyl group of the Neu5Ac residue receives the largest amount of saturation transfer in each of the compounds **3**−**5** and therefore was used as reference. A series of STD titration experiments delivered STD amplifications as a function of ligand excess (Figure 6), reflecting that within the *N*-acyl group of the Glc*N*Ac residue saturation transfer to H5 of the aromatic ring is most efficient for each of the compounds **3**−**5**.

Discussion

In this study, the combined use of surface plasmon resonance experiments, STD NMR experiments, and transferred NOE analyses furnishes details of the molecular recognition of the sLe^a epitope and various derivatives thereof by a monoclonal antibody, GSLA-2. Surface plasmon resonance experiments delivered a ranking of the structural variations and their relevance to the binding reaction of sLe^a to GSLA-2 in terms of their dissociation constants, K_D (Table 1). The comparison shows that the loss of the C6-methyl group of fucose is always associated with a decrease in binding affinity. Likewise, modifications of the *N*-acetyl group of the Glc*N*Ac residue in sLe^a resulted in reduced affinity and, at the extreme of substituting the Glc*N*Ac moiety with a cyclohexanediol ring (compound **7**), in a complete loss of binding.

The variation of the *N*-acyl substituents in compounds **2**−**5** shows that the *N*-acetyl group in sLe^a cannot simply be exchanged by other types of substituents to yield a better binding affinity. It appears that the *N*-acetyl group is already optimized for binding to GSLA-2, and since any modification results in at least a 10-fold increase in K_D (Table 1), it can be concluded that the *N*-acetyl group is essential for a good binding affinity. In addition, the lack of the C6-methyl group of the fucose residue in compounds **2** and **4** results in another substantial decrease of binding affinity, e.g., an almost 6-fold reduction when comparing compounds **3** and **4**. Consequently, compound **4**, which lacks the C6-methyl group of fucose and has a modified *N*-acyl side chain in the GlcNAc moiety, has the lowest binding affinity in this row of compounds, characterized by a ~150-fold increase in K_D compared to sLe^a. In this context it is also interesting to compare the 3,5-dihydroxybenzyl carbamate derivative **2** to the 3,4-dihydroxybenzyloxy derivative **4**. In both compounds the C6-methyl group of fucose is missing, resulting in a decreased affinity compared to the parent compound sLe^a (**1**). Interestingly, the introduction of two extra bonds between the CO function of the carbamate and the phenyl ring (compound **2**) leads to an increase in binding affinity. This may be explained by an increased flexibility of the *N*-acyl side chain, resulting in a better accommodation of this group within the binding pocket.

For sLe^x no binding activity was detected in the surface plasmon resonance experiments, although sLe^x is structurally closely related to sLe^a (Figure 1). It has been shown before that sLe^a and sLe^x may be superimposed by rotating one of the molecules 180° around the long axis (C1−C4) of the Glc*N*Ac pyranose ring and that the conformational properties of the tetrasaccharides sLe^a and sLe^x are very similar.[20] The major structural differences between sLe^a and sLe^x are summarized as follows. (1) When superimposed, the *N*-acetyl function of Glc*N*Ac of sLe^a is at the C6 position of GlcNAc in sLe^x

and vice versa. (2) The ring oxygen O5 of Glc*N*Ac in sLe^a is located at the position of C1 of Glc*N*Ac in sLe^x and vice versa. Assuming that the Neu5Ac, Gal, and Fuc residues of sLe^a and sLe^x bind to the same subsites of the GSLA-2 binding pocket, it is therefore concluded that the significantly decreased binding affinity of sLe^x is due to two major structural features. First, the *N*-acetyl group is missing at the correct position, where now a CH_2OH group is positioned. Second, the $O(CH_2)_8$-COOMe spacer is shifted relative to its position in the sLe^a ligand and thus creates potential steric conflicts with the amino acids of the binding pocket.

From Table 1 it is seen that the linear pentasaccharide LSTa (compound **8** in Figure 2) also binds to GSLA-2 with a K_D value similar to the one of compound **5**. It appears that that the two extra pyranose rings at the reducing end of LSTa add to the free energy of binding and thus compensate for the loss of fucose. Consistent with this explanation is the interpretation that the $-O-(CH_2)_8COOMe$ spacer in sLe^x is oriented such that it cannot contribute to the binding affinity and may even be in steric conflict with amino acids of the antigen binding site. In contrast to sLe^x, the *N*-acetyl function of Glc*N*Ac in LSTa is placed at the same position as for sLe^a. From these results it may be predicted that a fucosylated LSTa pentasaccharide would have a significantly increased binding affinity toward GSLA-2.

From the Biacore sensorgrams (Figure 3), it can be seen that a kinetics analysis is possible only for sLe^a, although at the limit of the kinetics resolution of the Biacore 3000 instrument. The on- and off-rates for the other derivatives were too fast to be followed with this instrument. The analysis reveals that k_{off} for sLe^a is about 0.5 s^{-1} and k_{on} is about 10^5 M^{-1} s^{-1}. Therefore, the association reaction is significantly slower, and this is expected for a diffusion-controlled association process. This can be explained to a large extent by the conformational flexibility of the neuramic acid residue.[31,34,36−40] It is reasonable to assume that upon binding, only one of the conformations present in aqueous solution is recognized by the antibody.[31] This conformational selection of the α(2,3)-glycosidic linkage during the binding process may be associated with a significant amount of activation entropy.

Complementary to the determination of dissociation constants K_D by surface plasmon resonance, the binding epitopes of sLe^a and its derivatives (Figure 2) were mapped at an atomic resolution using STD NMR.[8] One important observation is that each pyranose ring of sLe^a is involved in binding to GSLA-2, as all protons receive saturation transfer. Therefore, the antibody recognizes a tetrasaccharide epitope. Because good binding affinity for LSTa (compound **8**) may be explained by the extension of the binding epitope at the reducing end, one may conjecture that the $O(CH_2)_8COOMe$ spacer is also in contact with the binding pocket of GSLA-2. In fact, only very weak STD effects were observed for the spacer. Therefore, we suggest that the spacer makes only a loose contact with the binding site and as such contributes to the overall binding, yet not to the extent as the additional pyranose units in LSTa.

One has to be aware that the STD intensities in Table 2 depend on whether the on-resonance frequency for saturation transfer is set at a frequency in the region of aromatic amino acid side chain protons or in the region of aliphatic amino acid side chain protons. This is due to an effect termed "exchange leakage" that has been discussed in detail before.[28,29] In short, saturation that originates at aliphatic amino acid residues first has to be passed on to aromatic amino acids before it may be transferred to protons of the ligand that are in contact with aromatic amino acid protons and vice versa. Since the bound ligand molecules are in fast exchange with the bulk of free ligand molecules, saturation is effectively removed from the binding site protons, and the transfer of saturation within the protein via relay protons competes with the "leakage" of saturation into the pool of free ligand molecules. Whereas the transfer of saturation within the protein depends on the efficiency of spin diffusion, i.e., on the transverse relaxation time T_2, the exchange reaction is determined by the dissociation rate of the protein−ligand complex. Therefore, when the saturation transfer is indirect, i.e., it occurs via aromatic or aliphatic relay protons within the protein, it becomes dependent on the respective T_2 values and on k_{off}.[28,29] Only for very short T_2 times in the case of very large proteins is the difference negligible. This dependence on the saturation frequency may be put to good use in cases where a quantitative treatment of the STD data is aimed for. In contrast, direct saturation of amino acid protons in contact with ligand protons leads to more efficient saturation transfer because no relay protons in the protein are involved in this process, which is independent of individual spin diffusion pathways inside the protein.

In all experiments it is observed that both *N*-acetyl groups of sLe^a receive a large fraction of saturation transfer. Since the signals of the two *N*-acetyl groups are resolved at a lower temperature of 290 K, it was possible to discriminate between the two groups showing that the Glc*N*Ac *N*-acetyl function is in slightly more intimate contact (larger STD value) with binding site protons, independent of the saturation frequency. The protons H1, H4, and H5 of fucose, the protons H1, H3, and H4 of Gal and Glc*N*Ac, the proton H2 of Gal, and H6proS of Glc*N*Ac show larger relative STD intensities with the saturation frequency set at 6.7 ppm, indicating that this part of sLe^a makes contact with aromatic amino acids in the binding pocket. For the C6-methyl group of fucose the opposite situation is observed, and it is concluded that it is in contact with aliphatic amino acid residues. For the other protons the dependency on the saturation frequency is less pronounced.

Although surface plasmon resonance did not allow measurement of binding affinities for sLe^x, very weak binding affinity to GSLA-2 was observed in both transferred NOE experiments and STD NMR experiments. From the STD NMR data, it is concluded that the antibody recognizes mainly the neuramic acid residue. This is highlighted by the fact that no observable signal is found for the *N*-acetyl function of Glc*N*Ac in the STD spectrum. The Lewis^x core does not receive large amounts of saturation transfer (Table 2), thus substantiating the hypothesis that the $-O-(CH_2)_8COOMe$ spacer is in steric conflict with amino acids in the binding pocket. A comparison with other proteins that recognize sLe^a or sLe^x shows that this strong discrimi-

nation between the two epitopes is quite unique. For example, for E- and P-selectin, it has been observed that these lectins recognize both tetrasaccharides with similar affinities. From crystallographic studies of these complexes,[32,33] it is known that the binding pocket is rather flat. From NMR experiments and from chemical modifications it became apparent that the main binding epitope is represented by the fucose and the galactose units and only portions of the neuramic acid and the Glc*N*Ac residues. In contrast, our STD NMR data indicate that the complete tetrasaccharide is buried in the antigen-binding site of the GSLA-2. Therefore, most modifications of sLe^a do not lead to increased binding affinities toward GSLA-2.

To answer the question of whether sLe^x binds to the same site of GSLA-2 as sLe^a, competitive NOE (Figure 4) and STD NMR experiments (Figure 5) were performed. Since competition was observed, it is concluded that sLe^a and sLe^x indeed bind to the same site.

In general, our study highlights the benefits of combined STD NMR experiments and Biacore studies for the analysis of structure−activity relationships. Here, structural variations of the sLe^a epitope were correlated with binding affinities toward a monoclonal antibody GSLA-2, which is used in tumor diagnosis. The study has revealed the key pharmacophoric groups that are required for the recognition of this carbohydrate epitope by the antibody and has delivered the binding epitopes of sLe^a and derivatives thereof at atomic resolution.

Experimental Section

NMR Experiments and Sample Preparation. NMR experiments were performed on Bruker DRX 500 and DPX 360 spectrometers operating at 500 and 360 MHz, respectively. GSLA-2 belongs to the IgG1 subclass and has a molecular weight of 150 kDa. For the preparation of the GSLA-2/oligosaccharide samples, GSLA-2 was transferred into deuterated PBS buffer (20 mM phosphate, 10 mM sodium chloride) using Centricon (Amicon) or Vivaspin (Sartorius) concentrators with a molecular weight cutoff of 30 or 10 kDa, respectively. The pH was adjusted to 7.2−7.4 and was not corrected for D_2O. The GSLA-2/sLe^x samples each contained 2.8 mg of GSLA-2 in 560 μL of buffer solution, corresponding to 67 μM in binding sites. The GSLA-2/sLe^a and GSLA-2/**2** − **5** samples each contained 0.3 mg of GSLA-2 in 545 μL of buffer solution, corresponding to 7.4 μM in binding sites. Ligands were dissolved in D_2O and titrated into the GSLA-2 samples such that an addition of 10 μL of ligand solution corresponded to a binding site/ligand ratio of 1:20. The binding site/ligand ratio was varied from 1:20 to 1:200.

For 1D ^{1}H NMR experiments, 16K data points were accumulated with a spectral width of 10 ppm. The acquired data were subjected to exponential line broadening prior to Fourier transformation. Chemical shifts were referenced against DSS. The ^{1}H NMR signal assignment was achieved via the standard 2D experiments COSY, TOCSY, NOESY, and HSQC. For these spectra the quadrature detection method used in t_2 was the TPPI method except for the case of the HSQC spectra where the echo/antiecho method was used instead; the residual HDO was suppressed by weak preirradiation when required.

NOESY Experiments. NOE spectra were acquired with 512 increments in t_1 and 2K data points in t_2. The number of transients acquired per increment was sample-dependent. Prior to 2D Fourier transformation, the data matrix was zero-filled to 4K (t_2) × 2K (t_1) data points and multiplied by a $\pi/2$ shifted squared sine bell function in both dimensions. The NOE spectrum for the GSLA-2/sLe^x/sLe^a sample obtained at 360 MHz was acquired with 256 increments in t_1 and 2K data points in t_2. For this spectrum 16 transients were acquired for each increment.

STD NMR Experiments. STD NMR spectra were obtained on a Bruker DRX 500 spectrometer equipped with a triple resonance probehead, incorporating gradients in the *z*-axis. For the acquisition of STD NMR spectra, a 1D pulse sequence incorporating a $T_1\rho$ filter was used. On-resonance irradiation was performed at −1.0, 0.4, 6.7, or 7.2 ppm, and off-resonance was performed at −20 or 40 ppm. Irradiation was performed using 50 Gaussian pulses with a 1% truncation and 49 ms duration and were separated by a delay of 1 ms to give a total saturation time of 1 s. The duration of the $T_1\rho$ filter was 15 ms. STD NMR spectra were acquired with a total of 1024−4096 transients in addition to 32 scans to allow the sample to come to equilibrium. Spectra were obtained with a spectral width of 10 ppm and 16K data points. Reference spectra were acquired using the same conditions but with only half the number of transients. STD amplification factors were determined as previously described.

Surface Plasmon Resonance Experiments (Biacore). Surface plasmon resonance experiments were performed on a Biacore 3000 machine using CM5 chips. GSLA-2 was immobilized following the standard Biacore EDC/NHS immobilization procedure. For this, 2 μL of a GSLA-2 solution of 3.9 mg/mL in PBS buffer was added to 98 μL of acetate buffer, pH 4.5. The immobilization yielded between 12.000 and 20.000 resonance units. For a reference in one flow cell anti myoglobin antibody was immobilized, and one other flow cell was only capped with ethanol amine. Ligands were dissolved in HEPES buffer (10 mM Hepes, pH 7.4, 150 mM NaCl, and 0.005% (v/v) polysorbate 20, Biacore). Twelve ligand concentrations (for sLe^x, 16 ligand concentrations) ranging from 0.2 to 800 μM were used for the experiments. The flow rate was 5 μL/min for the immobilization and 10 μL/min for the injection of ligands. For the determination of K_D values and for the kinetics analysis, standard Biacore software, version 3.2, was used.

Acknowledgment. T.P. gratefully acknowledges support from the Deutsche Forschungsgemeinschaft (Grant SFB 470, Project B3; Grant Me 1830) and the Fonds der Chemischen Industrie. T.P. and B.E. thank the Volkswagen Stiftung (within the grant program "Conformational Control of Biomolecular Function"). Finally, T.P. and B.E. thank the University of Lübeck and the University of Basel, respectively, for generous support.

Appendix

Abbreviations. sLe^a = sialyl Lewis^a = tetrasaccharide **1**; sLe^x = sialyl Lewis^x = tetrasaccharide **6**; GSLA-2 = monoclonal antibody that recognizes sLe^a; mAb = monoclonal antibody; Glc*N*Ac = D-*N*-acetylglucosamine; Gal = D-galactose; Fuc = L-fucose; Neu5Ac = D-*N*-acetylneuramic acid = 5-acetamido-3,5-dideoxy-D-glycero-α-D-galacto-2-nonulopyranose; STD NMR = saturation transfer difference NMR; NOESY = nuclear Overhauser and exchange spectroscopy.

References

(1) Blattman, J. N.; Greenberg, P. D. Cancer Immunotherapy: A Treatment for the Masses. *Science* **2004**, *305*, 201−205.
(2) Bundle, D. R. Antibody−Oligosaccharide Interactions Determined by Crystallography. In *Glycosciences: Status and Perspectives*; Gabius, H.-J., Gabius, S., Eds.; Chapman and Hall: Weinheim, Germany, 1997; pp 311−331.
(3) Weimar, T.; Harris, S. L.; Pitner, J. B.; Bock, K.; Pinto, B. M. Transferred Nuclear Overhauser Enhancement Experiments Show That the Monoclonal Antibody Strep 9 Selects a Local Minimum Conformation of a *Streptococcus* Group A Trisaccharide-Hapten. *Biochemistry* **1995**, *34*, 13672−13680.

(4) Haselhorst, T.; Espinosa, J.-F.; Jiménez-Barbero, J.; Sokolowski, T.; Kosma, P.; Brade, H.; Brade, L.; Peters, T. NMR Experiments Reveal Distinct Antibody-Bound Conformations of a Synthetic Disaccharide Representing a General Structural Element of Bacterial Lipopolysaccharide Epitopes. *Biochemistry* **1999**, *38*, 6449−6459.
(5) Maaheimo, H.; Kosma, P.; Brade, L.; Brade, H.; Peters, T. Mapping the Binding of Synthetic Disaccharides Representing Epitopes of Chlamydial Lipopolysaccharide to Antibodies with NMR. *Biochemistry* **2000**, *39*, 12778−12788.
(6) Mayer, M.; Meyer, B. Characterization of Ligand Binding by Saturation Transfer Difference NMR Spectroscopy. *Angew. Chem., Int. Ed.* **1999**, *38*, 1784−1788.
(7) Vogtherr, M.; Peters, T. Application of NMR Based Binding Assays To Identify Key Hydroxy Groups for Intermolecular Recognition. *J. Am. Chem. Soc.* **2000**, *122,* 6093−6099.
(8) Mayer, M.; Meyer, B. Group Epitope Mapping by Saturation Transfer Difference NMR To Identify Segments of a Ligand in Direct Contact with a Protein Receptor. *J. Am. Chem. Soc.* **2001**, *123,* 6108−6117.
(9) Peters, T.; Meyer, B. NMR Techniques for Screening and Identifying Ligand Binding to Receptor Proteins. *Angew. Chem., Int. Ed.* **2003**, *42*, 864−890.
(10) Johnson, M. A.; Pinto, B. M. Saturation Transfer Difference 1D-TOCSY Experiments To Map the Topography of Oligosaccharides Recognized by a Monoclonal Antibody Directed against the Cell-Wall Polysaccharide of Group A Streptococcus. *J. Am. Chem. Soc.* **2002**, *124*, 15368−15374.
(11) Johnson, M. A.; Pinto, B. M. Saturation-Transfer Difference NMR Studies for the Epitope Mapping of a Carbohydrate-Mimetic Peptide Recognized by an Anti-Carbohydrate Antibody. *Bioorg. Med. Chem.* **2004**, *12*, 295−300.
(12) Magnani, J. L.; Brockhaus, M.; Smith, D. F.; Ginsburg, V.; Blaszczyk, M.; Mitchell, K. F.; Steplewski, Z.; Koprowski, H. A Monosialoganglioside Is a Monoclonal Antibody-Defined Antigen of Colon Carcinoma. *Science* **1981**, *212*, 55−56.
(13) Magnani, J. L.; Nilsson, B.; Brockhaus, M.; Zopf, D.; Steplewski, Z.; Koprowski, H.; Ginsburg, V. J. A Monoclonal Antibody-Defined Antigen Associated with Gastrointestinal Cancer Is a Ganglioside Containing Sialylated Lacto-*N*-Fucopentaose II. *Biol. Chem.* **1982***, 257,* 14365−14369.
(14) Takada, A.; Ohmori, K.; Takahashi, N.; Tsuyuoka, K.; Yago, K.; Zenita, K.; Hasegawa, A.; Kannagi, R. Adhesion of Human Cancer Cells to Vascular Endothelium Mediated by a Carbohydrate Antigen, Sialyl Lewis A. *Biochem. Biophys. Res. Commun.* **1991**, *179,* 713−719.
(15) Takada, A.; Ohmori, K.; Yoneda, T.; Tsuyuoka, K.; Hasegawa, A.; Kiso, M.; Kannagi, R. Contribution of Carbohydrate Antigens Sialyl Lewis A and Sialyl Lewis X to Adhesion of Human Cancer Cells to Vascular Endothelium. *Cancer Res.* **1993**, *53*, 354−361.
(16) Nakayama, T.; Watanabe, M.; Katsumata, T.; Teramoto, T.; Kitajima, M. Expression of Sialyl Lewis^a as a New Prognostic Factor for Patients with Advanced Colorectal Carcinoma. *Cancer* **1995**, *75,* 2051−2056.
(17) Nakagoe, T.; Sawai, T.; Tsuji, T.; Jibiki, M.; Ohbatake, M.; Nanashima, A.; Yamaguchi, H.; Yasutake, T.; Ayabe, H.; Arisawa, K. Prognostic Value of Serum Sialyl Lewis(a), Sialyl Lewis-(x) and Sialyl Tn Antigens in Blood from the Tumor Drainage Vein of Colorectal Cancer Patients. *Tumor Biol*. **2001**, *22*, 115−122.
(18) Gorrin, G.; Christensen, S.; Moore, M.; Trujillo, K.; Farwell, M.; Teramoto, Y.; Magnani, J. L. Comparison of the Chiron Diagnostics American Chemical Society:180 GI and Centocor CA19−9 assays by eptitope mapping and analytical and clinical performance. *Tumor Biol.* **1997**, *18*, p 79.
(19) Spohr, U.; Hindsgaul, O.; Lemieux, R. U. Molecular Recognition. II. The Binding of the Lewis b and Y Human Blood Group Determinants by the Lectin IV of *Griffonia simplicifolia*. *Can. J. Chem.* **1984**, *63*, 2644−2652.
(20) Berg, E. L.; Robinson, M. K.; Mansson, O.; Butcher, E. C.; Magnani, J. L. A Carbohydrate Domain Common to Both Sialyl Le^a and Sialytl Le^x Is Recognized by the Endothelial Cell Leukocyte Adhesion Molecule ELAM-1. *J. Biol. Chem.* **1991**, *266*, 14869−14872.
(21) Rich, R. L.; Myszka, D. G. Advances in Surface Plasmon Resonance Biosensor Analysis. *Curr. Opin. Biotechnol.* **2000**, *11*, 54−61.
(22) Morton, T. A.; Myszka, D. G. Kinetic Analysis of Macromolecular Interactions Using Surface Plasmon Resonance Biosensors. *Methods Enzymol.* **1998**, *295*, 268−294.
(23) Nagata, K.; Handa, H. *Real-Time Analysis of Biomolecular Interactions: Applications of Biacore*; Springer-Verlag, Berlin, 2000.
(24) Keller, R. M.; Wüthrich, K. Assignment of the Heme c Resonances in the 360 MHz H NMR Spectra of Cytochrome *c*. *Biochim. Biophys. Acta* **1978**, *533*, 195−208.
(25) Cayley, P. J.; Albrand, J. P.; Feeney, J.; Roberts, G. C.; Piper, E. A.; Burgen, A. S. Nuclear Magnetic Resonance Studies of the Binding of Trimethoprim to Dihydrofolate Reductase. *Biochemistry* **1979**, *18*, 3886−3895.
(26) Akasaka, K. Intermolecular Spin Diffusion as a Method for Studying Macromolecule−Ligand Interactions. *J. Magn. Reson.* **1979**, *36*, 135−140.
(27) Poppe, L.; Brown, G. S.; Philo, J. S.; Nikrad, P. V.; Shah, B. H. Conformation of sLe^x Tetrasaccharide, Free in Solution and Bound to E-, P-, and L-Selectin. *J. Am. Chem. Soc.* **1997**, *119*, 1727−1736.
(28) Jayalakshmi, V.; Krishna, N. R. CORCEMA Refinement of the Bound Ligand Conformation within the Protein Binding Pocket in Reversibly Forming Weak Complexes Using STD-NMR Intensities. *J. Magn. Reson*. **2004**, *168*, 36−45.
(29) Jayalakshmi, V.; Krishna, N. R. Complete Relaxation and Conformational Exchange Matrix (CORCEMA) Analysis of iNtermolecular Saturation Transfer Effects in Reversibly Forming Ligand−Receptor Complexes. *J. Magn. Reson.* **2002**, *155*, *106*−*118*.
(30) Jayalakshmi, V.; Biet, T.; Peters, T.; Krishna, N. R. Refinement of the Conformation of UDP-Galactose Bound to Galactosyltransferase Using the STD NMR Intensity-Restrained CORCEMA Optimization. *J. Am. Chem. Soc.* **2004**, *126*, 8610−8611.
(31) Scheffler, K.; Ernst, B.; Katopodis, A.; Magnani, J. L.; Wang, W. T.; Weisemann, R.; Peters, T. Determination of the Bioactive Conformation of the Carbohydrate Ligand in the E-Selectin/Sialyl Lewis^x Complex. *Angew. Chem., Int. Ed. Engl.* **1995**, *34*, 1841−1844.
(32) Somers, W. S.; Tang, J.; Shaw, G. D.; Camphausen, R. T. Insights into the Molecular Basis of Leukocyte Tethering and Rolling Revealed by Structures of P- and E-Selectin Bound to SLe(X) and PSGL-1. *Cell* **2000**, *103,* 467−479.
(33) Graves, B. J.; Crowther, R. L.; Chandran, C.; Rumberger, J. M.; Li, S.; Huang, K. S.; Presky, D. H.; Familletti, P. C.; Wolitzky, B. A.; Burns, D. K. Insight into E-sElectin/Ligand Interaction from the Crystal Structure and Mutagenesis of the lec/EGF Domains. *Nature* **1994**, *367*, 532−538.
(34) Kogelberg, H.; Frenkiel, T. A.; Homans, S. W.; Lubineau, A.; Feizi, T. Conformational Studies on the Selection and Natural Killer Cell Receptor Ligands Sulfo- and Sialyl-lacto-*N*-fucopentaoses (SuLNFPII and SLNFPII) Using NMR Spectroscopy and Molecular Dynamics Simulations. Comparisons with the Nonacidic Parent Molecule LNFPII. *Biochemistry* **1996**, *35*, 1954−1964.
(35) Bechtel, B.; Wand, A. J.; Wroblewski, K.; Koprowski, H.; Thurin, J. Conformational Analysis of the Tumor-Associated Carbohydrate Antigen 19-9 and Its Le^a Blood Group Antigen Component as Related to the Specificity of Monoclonal Antibody CO19-9. *J. Biol. Chem.* **1990**, 2028−2037.
(36) Miller, K. E.; Mukhopadhyay, C.; Cagas, P.; Bush, C. A. Solution Structure of the Lewis x Oligosaccharide Determined by NMR Spectroscopy and Molecular Dynamics Simulations. *Biochemistry* **1992**, *31*, 6703−6709.
(37) Haselhorst, T.; Weimar, T.; Peters, T. Molecular Recognition of Sialyl Lewis^x and Related Saccharides by Two Lectins. *J. Am. Chem. Soc.* **2001**, *123*, 10705−10714.
(38) Mukhopadhyay C.; Bush C. A. Molecular Dynamics Simulation of Oligosaccharides Containing *N*-Acetyl Neuraminic Acid. *Biopolymers* **1994**, *34*, 11−20.
(39) Lin, Y.-C.; Hummel, C. W.; Huang, D.-H.; Ichikawa, Y.; Nicolaou, K. C.; Wong, C.-H. Conformational Studies of Sialyl Lewis X in Aqueous Solution. *J. Am. Chem. Soc.* **1992**, *114*, 5452−5454.
(40) Sabesan, S.; Bock, K.; Paulson, J. Conformational Analysis of Sialyloligosaccharides. *Carbohydr. Res.* **1991**, *218,* 27−54.
(41) Baisch, G.; Öhrlein, R.; Streiff, M.; Enzymatic Fucosylation of Non-Natural Sialylated Type-1 Trisaccharides with Recombinant Fucosyltransferase-III. *Bioorg. Med. Chem. Lett.* **1998**, *8*, 161−164.
(42) Baisch, G.; Öhrlein, R.; Streiff, M.; Kolbinger, F. Enzymatic Synthesis of Sialyl Lewis^a-Libraries with Two Non-Natural Monosaccharide Units. *Bioorg. Med. Chem. Lett.* **1998**, *8*, 755−758.
(43) Öhrlein, R.; Baisch, G.; Katopodis, A.; Streiff, M.; Kolbinger, F. Transferase-Catalyzed Synthesis of Non-Natural Oligosaccharide Libraries (sLe^a- and sLe^x-Analogues). *J. Mol. Catal. B: Enzym.* **1998**, *5*, 125−127.
(44) Ernst, B.; Wagner, B.; Baisch, G.; Katopodis, A.; Winkler, T.; Öhrlein, R. Substrate Specificity of Fucosyltransferase III: An Efficient Synthesis of Sialyl Lewis^x, Sialyl Lewis^a-Derivatives and Mimetics Thereof. *Can. J. Chem.* **2000**, *78*, 892−904 and references therein.

JM0502687